Energy Consumption Minimization with Throughput Heterogeneity in Wireless-Powered Body Area Networks

Tong Wang, *Member, IEEE,* Yang Shen, Lin Gao, *Senior Member, IEEE,* Yufei Jiang, *Member, IEEE,* Ting Ma, *Member, IEEE,* and Xu Zhu, *Senior Member, IEEE*

***Abstract*—In this paper, we focus on a wireless-powered body area network in which the simultaneous wireless information and power transfer (SWIPT) technique is adopted. We consider two scenarios based on whether sensor nodes (SNs) are equipped with battery. For the first time, energy consumption minimization with throughput heterogeneity (ECM-TH) problem is addressed for both scenarios. For the battery-free scenario, a low-complexity time allocation scheme is proposed. This scheme solves the ECM-TH problem based on a hybrid method of gradient descent and bisection search algorithms. Consequently, compared with the interior-point method, our scheme has a lower computational complexity for the same energy consumption performance of the network. For the battery-assisted scenario, the non-convex ECM-TH problem is first transformed into a convex optimization problem by introducing auxiliary variables. Then, a joint time and power allocation scheme based on the Lagrange dual subgradient method is proposed to solve it. Compared with the battery-free scenario, the energy consumption and outage probability are both decreased in the battery-assisted scenario. Moreover, we address a special case wherein the feasible set of the abovementioned ECM-TH problems may be empty owing to poor channel conditions or high throughput requirements of SNs.**

***Index Terms*—Wireless-powered body area networks, SWIPT, energy consumption minimization, throughput heterogeneity, resource allocation.**

I. Introduction

FIFTH generation (5G) communication technology is being deployed globally owing to its capability of supporting high speed, low latency, and increased connectivity. Furthermore, widespread 5G will greatly promote the development of 5G-enabled Internet of Things (IoT), which introduces the advantages of 5G into the communication of IoT [1]. As an application scenario of 5G-enabled IoT, wireless body area networks (WBANs) have been developed in recent years [2], [3]. Considering that sensor nodes (SNs) in a WBAN need to operate for a long duration, wireless-powered body area networks (WP-BANs) have received considerable research interest. WP-BANs introduce the energy harvesting (EH) transmission techniques into WBANs to ensure a stable energy supply. There are three main EH transmission techniques: wireless power transfer (WPT), wireless-powered communication network (WPCN) and simultaneous wireless information and power transfer (SWIPT) [4]. In the WPT technique, the transmitter transfers the energy only to the receiver. In the WPCN technique, the transmitter first transfers the energy to the receiver and then the receiver transmits the data to the transmitter. Compared with the WPT and WPCN techniques, the SWIPT technique allows the transmitter to transmit information and energy concurrently to receivers, yielding higher information-energy transmission efficiency and lower energy consumption [4], [5].

Many efforts have been made to promote the system performance of the radio-frequency (RF) EH-aided networks by optimizing resource allocation. The authors of [6]–[13] investigated the EH networks in which the nodes were not equipped with batteries (i.e., battery-free scenarios). In [6]–[8], the authors investigated the sum-throughput maximization (STM) problem. By solving the STM problem, the sum of the throughput of all the nodes can be maximized. However, this solution may lead to extremely unfair allocation of throughput for nodes that are far from the hybrid access point (HAP) due to the "doubly near-far" problem. In [6], the authors investigated the common-throughput maximization (CTM) problem. The goal of the study was to maximize the minimal achievable throughput of all the nodes to overcome the "doubly near-far" problem. By solving the CTM problem, the throughput allocation of all the nodes is relatively fair, while the sum throughput decreases. To achieve both relatively good throughput performance and fair throughput allocation, authors in [9] proposed a sum-utility maximization (SUM) scheme based on the marginal utility theory [14], in which the logarithmic sum of throughput of all the nodes was maximized. Moreover, some researchers have investigated various solutions for the resource allocation of battery-free scenarios, aiming at optimizing the energy efficiency [10], [11], reliable communication probability [12], and transmission completion time [13]. In contrast, some researchers have investigated

This work was supported in part by the National Natural Science Foundation of China under Grants 61801145, 61972113, and 61901138, in part by Shenzhen Science and Technology Program under Grants JCYJ20180306171800589, JCYJ20190806112215116, and KQTD20190929172545139, in part by the Natural Science Foundation of Guangdong Province under Grant 2018A030313344 and 2018A030313298, in part by the National Key Research and Development Program of China under Grant 2018YFC1312000, and in part by the Guangdong Science and Technology Planning Project 2018B030322004. *(Corresponding authors: Yufei Jiang and Lin Gao.)*

T. Wang, Y. Shen, L. Gao, and Y. Jiang are with Harbin Institute of Technology, Shenzhen, China (e-mail: tongwang@hit.edu.cn; 18s152614@stu.hit.edu.cn; gaol@hit.edu.cn; jiangyufei@hit.edu.cn).

T. Ma is with Harbin Institute of Technology, Shenzhen, China, and also with Peng Cheng Laboratory, Shenzhen, China (e-mail: tmahit@outlook.com).

X. Zhu is with Department of Electrical Engineering and Electronics, University of Liverpool, Liverpool, UK (e-mail: xuzhu@liverpool.ac.uk).

EH networks where the nodes were equipped with batteries (i.e., battery-assisted scenarios) [15]–[18]. In [15], the authors investigated the tradeoff between energy consumption and transmission delay by utilizing the Lyapunov optimization theory. In [16] and [17], the authors proposed a joint power and time allocation method to achieve the maximum energy efficiency. In [18], the authors investigated the weighted STM problem in full-duplex EH networks.

However, none of the abovementioned studies considered the constraints of node throughput heterogeneity, which is an important constraint of SNs in WBANs. In a WBAN, each SN is responsible for monitoring one part of the human body and hence has different throughput requirements. For example, in a health-monitoring WBAN, the SNs required for monitoring the glucose level, electrocardiogram, and electroencephalogram have different throughput requirements that may vary from 1 kbps to 10 Mbps [3]. In [19]–[22], the authors considered node throughput heterogeneity. However, [19] and [20] ignored the circuit energy consumption. This is not reasonable for the WBAN scenario in which the circuit energy consumption is non-negligible compared with the communication energy consumption [16]. There were no constraints on the transmission power of the nodes in [19]–[22], which is not reasonable for WP-BANs as a high transmission power of SNs may have harmful effects on human health [11], [23], [24]. In addition, very few studies have paid attention to the energy consumption of the hybrid access point (HAP). In general, HAP in a WP-BAN is equipped with a finite battery, and all the consumed energy of SNs is obtained from the HAP. Therefore, to extend the service time of the HAP and simultaneously improve the user quality-of-experience, it is vital to decrease the energy consumption of the HAP in WP-BANs.

In this work, we focus on a WP-BAN that has a multi-antenna HAP and a number of single-antenna SNs. We consider the node throughput heterogeneity, circuit energy consumption, and transmission power limitations of SNs. By adopting the beamforming and SWIPT techniques, we formulate the energy consumption minimization with throughput heterogeneity (ECM-TH) problems under two WP-BAN scenarios: battery-free scenario and battery-assisted scenario. In the battery-free scenario, each SN does not have batteries. This is suitable for WP-BANs with SN size limitations, such as the SNs implanted in the human body. To avoid energy wastage, each SN would need to exhaust all the harvested energy on communication in each time slot. We prove that the ECM-TH problem of the battery-free WP-BAN is a convex optimization problem. The interior-point method [25] is used to solve the convex optimization problems by introducing barrier functions. However, the computational complexity of the solution is high because the interior-point method is used, which iterates hundreds of times when the primal and dual solutions are updated during each time slot. Therefore, according to the convexity of the problem, we propose a low-complexity time allocation scheme that solves the ECM-TH problem efficiently using a hybrid method that combinies the gradient descent (GD) [25] and bisection search (BS) algorithms [26]. In the GD algorithm, the objective function moves in the direction of descent in each iteration. In the BS algorithm, the length of the interval where the objective function is located is reduced by half in each iteration. In the proposed resource allocation scheme, the feasible set is first determined using the GD algorithm. Then, we use the BS algorithm to find the optimal solutions from the feasible set. In the battery-assisted scenario, each SN is equipped with a battery to store the harvested energy from the HAP. This setup is more suitable for WP-BANs in which SNs are deployed on the surface of the human body. The non-convex ECM-TH problem is first transformed into a convex optimization problem by introducing auxiliary variables. Then, we propose a resource allocation scheme for solving the transformed problem based on Lagrange dual subgradient method [25], which is a common method for solving the convex optimization problems through updating Lagrange multipliers iteratively. Considering the special case wherein the feasible set of the ECM-TH problem is empty owing to the poor channel conditions or high throughput requirements of SNs, we introduce a corresponding method based on the GD algorithm to address this case in the proposed resource allocation scheme in both scenarios. The major novelties of this paper are summarized as follows:

(1) To the best of our knowledge, this is the first study that investigates the ECM-TH problems in a WP-BAN where the circuit energy consumption and transmission power limitations of SNs are considered. Compared with the STM, CTM, and SUM schemes, energy consumption of our proposed schemes is much lower in both battery-free and battery-assisted scenarios.
(2) In the battery-free scenario, the proposed hybrid method can achieve the same energy consumption performance as the interior-point method but with a lower computational complexity.
(3) In the battery-assisted scenario, a joint time and power allocation scheme based on Lagrange dual subgradient method is proposed, resulting in lower energy consumption and outage probability compared with those in the battery-free scenario.
(4) Being different from the existing resource allocation schemes for WP-BANs, the special cases of the empty feasible set in the ECH-TH problem are considered and addressed in both scenarios, which makes the proposed resource allocation schemes more feasible.

The rest of this paper is organized as follows. In Section II, the system models of battery-free and battery-assisted WP-BANs are described. In Section III, the ECM-TH optimization problem in battery-free WP-BAN is formulated, and an efficient time allocation scheme is proposed to solve it. In Section IV, a joint time and power allocation scheme is proposed to solve the ECM-TH problem in battery-assisted WP-BAN. The simulation results are presented in Section V. Finally, Section VI concludes this paper. The list of acronyms and notations used in the paper are summarized in Table I and Table II.

II. WP-BAN System Model

The system contains one multi-antenna HAP with K antennas, N single-antenna SNs and cloud. As recommended by IEEE 802.15.6 [27], a star topology is adopted between

the communication links of the HAP and the SNs. The HAP is responsible for broadcasting RF energy and resource allocation information to all SNs, while SNs are in charge of transmitting sensory data to the HAP. The cloud is responsible for collecting data from the HAP for further utilization such as health monitoring. The WP-BAN model in this paper is shown in Fig. 1.

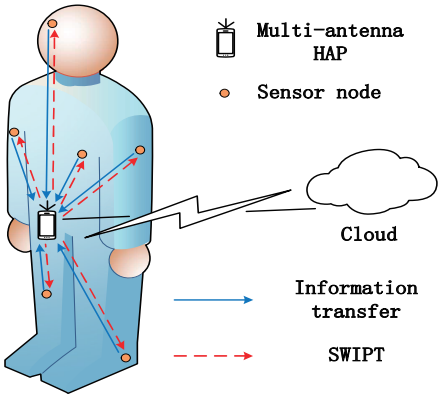

Fig. 1. WP-BAN with a multi-antenna HAP and single-antenna SNs.

The adopted transmission protocol is shown in the lower part of Fig. 2 which is time-slotted. The length of each time slot is T, which is divided into two phases: energy transmission (ET) phase and information transmission (IT) phase. During the ET phase, the HAP broadcasts RF power and resource allocation information to all SNs through SWIPT technique within time duration of $\tau_0 T$. The weighted linear multi-antenna beamforming technique [4] is applied at the HAP to improve the signal-to-noise ratio (SNR) at the receivers. During the IT phase, each SN i forwards its sensory data to the HAP within time duration of $\tau_i T$. Here, τ_0 and τ_i are respectively allocated time ratio for the ET phase and IT phase of the ith SN.

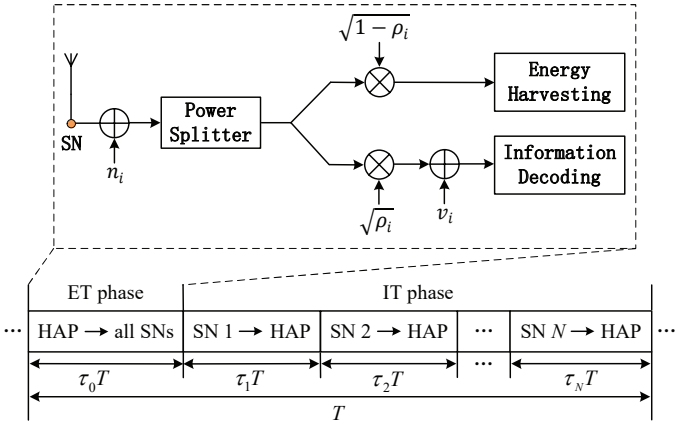

Fig. 2. Transmission protocol of the WP-BAN and PS architecture of SNs.

A. ET Phase

The SWIPT and weighted linear multi-antenna beamforming techniques are adopted at the HAP during ET phase. The transmitted vector $\mathbf{x}$ is expressed as

$$\mathbf{x} = \sqrt{P}\sum_{i=1}^{N}\mathbf{w}_i s, \tag{1}$$

where P is transmission power at the HAP which is bounded by $P_{\max}$. s denotes the normalized resource allocation information for broadcasting to all SNs. The maximum ratio transmission (MRT) beamforming can maximize the SNR at each SN for ID leading to more energy used for IT [11]. In addition, the MRT beamforming requires only the knowledge of channel conditions and its computational complexity is extremely low [28], which is suitable for the WP-BANs. Therefore, the MRT beamforming is adopted in this paper. The beamforming weights vector of MRT for the ith SN $\mathbf{w}_i$ is given by

$$\mathbf{w}_i = \frac{1}{\sqrt{N}}\frac{\mathbf{h}_i^{\mathrm{T}}}{||\mathbf{h}_i||}, \forall i \in \mathcal{N}_s, \tag{2}$$

where $\mathbf{h}_i = [h_{i,1}, h_{i,2}, \cdots, h_{i,K}]$ is the channel vector from the HAP to the ith SN, and $h_{i,j}$ is the channel coefficient from the jth antenna of the HAP to the ith SN. The operator $(\cdot)^{\mathrm{T}}$ denotes the matrix transpose. $\mathcal{N}_s = \{1, 2, \cdots, N\}$ is the set of all SNs. In addition, we assume that channel vectors between SNs and the HAP are quasi-static [25], that is, the elements in $\mathbf{h}_i(t)$ stay unchanged within one time slot, but may vary from one time slot to another. The received signals at the ith SN from the HAP are

$$y_i = \mathbf{h}_i\mathbf{x} + n_i, \forall i \in \mathcal{N}_s, \tag{3}$$

where $n_i \sim \mathcal{CN}(0, \sigma_i^2)$ is the additive white Gaussian noise (AWGN) introduced by the receiving antenna at the ith SN. σ_i^2 can be calculated by $\sigma_i^2 = \widehat{K}WT_0 \times 10^{F_i/10}$ as in [11], where $\widehat{K} = 1.3806503 \times 10^{-23}$ is the Boltzmann constant, W is the channel bandwidth in Hz, T_0 is the body temperature in kelvin, and F_i is the noise factor of the ith SN in dB.

The received signal power at the ith SN is divided between information decoding (ID) and EH with a splitting factor $0 < \rho_i < 1$ by using the power splitting (PS) architecture [4] which is shown in the upper part of Fig. 2. In detail, for the ith SN, ρ_i percent of the received signal power is utilized to ID, and the remaining power is used to transmit sensory data to the HAP. Thus, the signal for ID at the ith SN is modeled as

$$\begin{aligned}\widehat{y_i} &= \sqrt{\rho_i}\left(\mathbf{h}_i\mathbf{x} + n_i\right) + v_i \\ &= \sqrt{\rho_i}\left(\sum_{j=1}^{N}\sqrt{P}\mathbf{h}_i\mathbf{w}_j s + n_i\right) + v_i, \forall i \in \mathcal{N}_s,\end{aligned} \tag{4}$$

where $v_i \sim \mathcal{CN}(0, \delta_i^2)$ is the AWGN introduced by RF to baseband conversion at the ith SN. Based on (4), the SNR level for ID at the ith SN is expressed as

$$\gamma_i = \frac{\rho_i P\sum_{j=1}^{N}|\mathbf{h}_i\mathbf{w}_j|^2}{\rho_i\sigma_i^2 + \delta_i^2}, \forall i \in \mathcal{N}_s. \tag{5}$$

Similar to (4), the received signal for EH is given by

$$\widetilde{y_i} = \sqrt{1-\rho_i}\left(\sum_{j=1}^{N}\sqrt{P}\mathbf{h}_i\mathbf{w}_j s + n_i\right), \forall i \in \mathcal{N}_s. \tag{6}$$

TABLE I
TABLE OF ACRONYMS

Abbr.	Content	Abbr.	Content
5G	Fifth generation	MRT	Maximum ratio transmission
AWGN	Additive white gaussian noise	PS	Power splitting
BS	Bisection search	RF	Radio-frequency
CTM	Common-throughput maximization	SNR	Signal-to-noise ratio
ECM-TH	Energy consumption minimization with throughput heterogeneity	SNs	Sensor nodes
EH	Energy harvesting	STM	Sum-throughput maximization
ET	Energy transmission	SUM	Sum-utility maximization
GD	Gradient descent	SWIPT	Simultaneous wireless information and power transfer
HAP	Hybrid access point	WBANs	Wireless body area networks
ID	Information decoding	WP-BANs	Wireless-powered body area networks
IoT	Internet of things	WPCN	Wireless powered communication network
IT	Information transmission	WPT	Wireless power transfer

TABLE II
TABLE OF NOTATIONS

Symbol	Definition	Symbol	Definition
$\mathcal{N}_s$	Set of all SNs	$\mathbf{h}_i \in \mathbb{C}^{1\times K}$	Channel vector from the HAP to the ith SN
T	Length of time slot	$\mathbf{g}_i \in \mathbb{C}^{1\times K}$	Channel vector from the ith SN to the HAP
N	Number of SNs	$\mathbf{w}_i \in \mathbb{C}^{K\times 1}$	Beamforming weights vector
K	Number of antennas in the HAP	$\mathbf{x} \in \mathbb{C}^{\mathrm{K}\times 1}$	Transmitted data vector
W	Channel bandwidth	τ_i	Allocated time ratio for the IT phase for ith SN
s	Normalized resource allocation information	τ_0	Allocated time ratio for the ET phase
ρ_i	Splitting factor for ith SN in SWIPT technique	η	Energy conversion efficiency
γ_i	SNR level for ID at the ith SN	γ_0	SNR threshold for SNs to decode resource allocation information
R_i	Throughput of the ith SN during one time slot	D_i	Throughput requirement of the ith SN
p_i	Transmission power of the ith SN	p_{max}	Maximum transmission power of SNs
P	Transmission power of the HAP	P_{max}	Maximum transmission power of the HAP
B_{max}	Battery capacity of SNs	B_i	Achievable energy of the ith SN at the beginning of the time slot
d_i	Distance between the ith SN and the HAP	E_i	Harvested energy at the ith SN during the ET phase
$L(d_0)$	Path loss at the reference distance d_0	$\psi_{i,j}$	Body shadowing loss margin between the ith SN and the jth antenna
δ	Path loss exponent	$\xi_{i,j}$	Small-scale fading power gain between the ith SN and the jth antenna
μ	Step size in GD algorithm	δ_i^2	AWGN power introduced by RF to baseband conversion at the ith SN
w_i	Transmission priority weight of ith SN	σ_i^2	AWGN power introduced by the receiving antenna at the ith SN
α	Circuit energy consumption factor	σ_a^2	AWGN power introduced by receiving antenna at the HAP
$\widehat{K}$	Boltzmann constant	π_i	Probability of the ith SN being ignored
V_i	Product of τ_i and p_i	$r(\tau_0)$	Allocated sum ratios of one time slot T for a given τ_0
$\mathcal{L}$	Lagrange function of problem $\mathbf{P5}$	Δ_n	Step size of the nth iteration on updating Lagrange multipliers

Energy harvested from the receiver noise n_i is negligible since its power level is much lower than P [19]. Based on the received signal for EH in (6), the harvested energy at the ith SN during the ET phase of each time slot is calculated by

$$E_i = \tau_0 T\eta\mathbb{E}\{|\widetilde{y}_i|^2\} = \tau_0 T\eta(1-\rho_i)P\sum_{j=1}^{N}\left|\mathbf{h}_i\mathbf{w}_j\right|^2, \forall i \in \mathcal{N}_s, \tag{7}$$

where $\mathbb{E}\{\cdot\}$ denotes the expectation operator, and η denotes energy conversion efficiency.

B. IT Phase

1) IT phase of the battery-free scenario: In the battery-free scenario, each SN consumes all harvested energy during each time slot. In addition, compared with the energy consumption for IT, the circuit energy consumption of SNs is non-negligible [16]. The energy consumption ratio of IT to circuit is fixed at $\frac{\alpha}{1-\alpha}$ [13], i.e., each SN consumes αE_i of energy for IT during $\tau_i T$ and the rest for circuit energy consumption, where α is a fixed ratio for harvested energy of IT. Thus, the transmission power p_i of the ith SN can be expressed as

$$p_i = \frac{\alpha E_i}{\tau_i T} = \frac{\alpha\tau_0\eta(1-\rho_i)P\sum_{j=1}^{N}\left|\mathbf{h}_i\mathbf{w}_j\right|^2}{\tau_i}, \forall i \in \mathcal{N}_s. \tag{8}$$

In order to avoid electromagnetic emissions which is harmful to human health [11], we bound up the transmission power of SNs by $p_{\max}$, i.e.,

$$p_i \le p_{\max},\ \forall i \in \mathcal{N}_s. \tag{9}$$

Besides, to simplify the expression of the throughput of the SNs, we define

$$\theta_i = \frac{\alpha\eta}{\sigma_a^2}\sum_{j=1}^{N}\left|\mathbf{h}_i\mathbf{w}_j\right|^2\left|\left|\mathbf{g}_i\right|\right|^2, \forall i \in \mathcal{N}_s, \tag{10}$$

where σ_a^2 is AWGN power introduced by receiving antenna at the HAP, $\mathbf{g}_i = [g_{1,i}, g_{2,i}, \cdots, g_{K,i}]$ denotes the channel vector from the ith SN to the HAP. In addition, it is assumed that channel reciprocity holds in each time slot [11], [29], i.e., $\mathbf{g}_i = \mathbf{h}_i$. Then, according to Shannon-Hartley theorem [30],

the throughput of the ith SN in the battery-free scenario can be calculated by

$$R_i = \tau_i T W \log_2 \left[1 + \frac{\theta_i \tau_0 (1-\rho_i) P}{\tau_i}\right], \forall i \in \mathcal{N}_s. \quad (11)$$

2) IT phase of the battery-assisted scenario: In the battery-assisted scenario, each SN is equipped with a finite battery with initial energy of B_0 to store energy for IT which capacity is bounded by $B_{\max}$. As in the battery-free scenario, each SN consumes $\tau_i T p_i$ amount of energy for IT during $\tau_i T$ and $\frac{1-\alpha}{\alpha}\tau_i T p_i$ amount of energy for circuit energy consumption, i.e., α percent of consumed energy of each SN is utilized by IT and the rest energy is consumed for circuit. Thus, each SN consumes $\frac{1}{\alpha}\tau_i T p_i$ amount of energy on communication and circuit. Then, all SNs should follow the energy causality constraint at each time slot as follows:

$$\frac{1}{\alpha}\tau_i T p_i \le B_i + E_i, \ \forall i \in \mathcal{N}_s, \quad (12)$$

where p_i is transmission power of the ith SN which is bounded by $p_{\max}$ as in (9), and B_i is achievable energy of the ith SN at the beginning of the time slot. We denote $B_i(t)$ as the achievable energy of the ith SN at the beginning of the time slot t, which can be obtained by the following recursive equation:

$$B_i(t+1) = B_i(t) - \frac{1}{\alpha}\tau_i(t) T p_i(t) + E_i(t), \forall i \in \mathcal{N}_s. \quad (13)$$

Moreover, to avoid energy waste caused by overflow, we have

$$B_i + E_i \le B_{\max}, \ \forall i \in \mathcal{N}_s. \quad (14)$$

According to Shannon-Hartley theorem [30], the throughput of the ith SN in the battery-assisted scenario can be calculated by

$$R_i = \tau_i T W \log_2 \left(1 + \frac{p_i \left|\left|\mathbf{g}_i\right|\right|^2}{\sigma_a^2}\right), \forall i \in \mathcal{N}_s. \quad (15)$$

III. ECM-TH Problem in Battery-Free WP-BANS

A. Problem Formulation

In the battery-free WP-BAN model, SNs exhaust all energy harvested from the HAP during each time slot. Thus, the ECM-TH problem can be formulated as follows

$$\begin{aligned} \mathbf{P1}: & \min_{\tau_0, \boldsymbol{\tau}, \boldsymbol{\rho}, P} \tau_0 T P \\ s.t. \ & C1: R_i \ge D_i, \ \forall i \in \mathcal{N}_s \\ & C2: \gamma_i \ge \gamma_0, \ \forall i \in \mathcal{N}_s \\ & C3: 0 \le p_i \le p_{\max}, \ \forall i \in \mathcal{N}_s \\ & C4: 0 \le P \le P_{\max} \\ & C5: \sum_{i=0}^{N} \tau_i \le 1 \\ & C6: \tau_0 \ge 0, \tau_i \ge 0, \ \forall i \in \mathcal{N}_s \end{aligned} \quad (16)$$

where $\boldsymbol{\tau} = \{\tau_1, \tau_2 \cdots, \tau_N\}$ and $\boldsymbol{\rho} = \{\rho_1, \rho_2 \cdots, \rho_N\}$. D_i in constraint $C1$ is the throughput requirement of the ith SN. γ_0 in constraint $C2$ is the SNR threshold for SNs to decode resource allocation information correctly from the HAP. Constraints $C3$ and $C4$ are the transmission power limitation of SNs and the HAP. $C5$ and $C6$ are the constraints on time ratios for the ET and IT phases.

By substituting (5) into constraint $C2$, we can obtain

$$\frac{\rho_i P \sum_{j=1}^{N} \left|\mathbf{h}_i \mathbf{w}_j\right|^2}{\rho_i \sigma_i^2 + \delta_i^2} \ge \gamma_0, \forall i \in \mathcal{N}_s. \quad (17)$$

By rearranging (17), the following inequation on ρ_i is achieved:

$$\rho_i \ge \frac{\gamma_0 \delta_i^2}{P \sum_{j=1}^{N} \left|\mathbf{h}_i \mathbf{w}_j\right|^2 - \gamma_0 \sigma_i^2}, \forall i \in \mathcal{N}_s. \quad (18)$$

Considering that our goal is to minimize the sum energy consumption when all SNs meet the throughput requirements, each SN should spend more energy on IT and less energy on ID, which means that SN i should adopt a minimum PS factor ρ_i under the constraint $C2$. Thus, the ith SN's optimal PS factor ρ_i^* is equal to the right-hand side of (18), i.e.,

$$\rho_i^* = \frac{\gamma_0 \delta_i^2}{P \sum_{j=1}^{N} \left|\mathbf{h}_i \mathbf{w}_j\right|^2 - \gamma_0 \sigma_i^2}, \forall i \in \mathcal{N}_s. \quad (19)$$

Since the energy consumption of SN for IT is positively correlated with throughput and our target is minimizing total energy consumption, SN i should only transmit the required amount of data D_i. Thus, the inequality becomes equality for the constraint $C1$ in problem $\boldsymbol{P1}$. Then, by substituting (11) and the optimal PS factor ρ_i^* into constraint $C1$, we can obtain:

$$\tau_i T W \log_2 \left(1 + \frac{\widetilde{\theta}_i \tau_0 P}{\tau_i}\right) = D_i, \forall i \in \mathcal{N}_s, \quad (20)$$

where $\widetilde{\theta}_i = \theta_i(1-\rho_i^*)$. By rearranging (20), we can get the following equation:

$$\tau_0 T P = \frac{\tau_i T}{\widetilde{\theta}_i}\left(2^{\frac{D_i}{\tau_i T W}} - 1\right), \forall i \in \mathcal{N}_s. \quad (21)$$

We denote E_i^a as the demand of the ith SN for the energy supply of the HAP, i.e., the right-hand side of (21):

$$E_i^a \triangleq \frac{\tau_i T}{\widetilde{\theta}_i}\left(2^{\frac{D_i}{\tau_i T W}} - 1\right), \forall i \in \mathcal{N}_s. \quad (22)$$

Since formula (22) holds for all SNs. We can achieve that:

$$E_1^a = E_2^a = \cdots = E_N^a = \tau_0 T P, \quad (23)$$

which means that when we obtain the optimal solutions, all SNs should have the same demand for the HAP's energy supply, i.e., formula (23) is a necessary condition for obtaining the optimal solutions.

Lemma 1. *E_i^a is a monotonically decreasing function with respect to τ_i under the constraint of $C1$, where $0 \le \tau_i \le 1$.*

Proof. The derivative of E_i^a with respect to τ_i is

$$\begin{aligned} \frac{dE_i^a}{d\tau_i} &= \frac{T}{\widetilde{\theta}_i}\left(2^{\frac{D_i}{\tau_i T W}} - 1\right) - \frac{T}{\widetilde{\theta}_i} \cdot 2^{\frac{D_i}{\tau_i T W}} \cdot \frac{D_i}{\tau_i T W} \cdot \ln 2 \\ &= \frac{T}{\widetilde{\theta}_i}\left(2^{\frac{D_i}{\tau_i T W}} - 2^{\frac{D_i}{\tau_i T W}} \cdot \frac{D_i}{\tau_i T W} \cdot \ln 2 - 1\right) \\ &= \frac{T}{\widetilde{\theta}_i}\left(x_i - x_i \ln x_i - 1\right), \end{aligned} \quad (24)$$

where $x_i = 2^{\frac{D_i}{\tau_i TW}}$ which is greater than 1. Since the inequality $x_i - x_i \ln x_i - 1 < 0$ holds for any $x_i > 1$, we have $dE_i^a/d\tau_i < 0$. Thus, E_i^a is a monotonically decreasing function with respect to τ_i. The proof completes. □

Lemma 2. *The optimal transmission power of the HAP P^* in ECM-TH problem* $\mathbf{P1}$ *is equal to* $P_{\max}$.

Proof. We prove it by contradiction. Assume there is an optimal transmission power of the HAP $P^* < P_{\max}$. We denote $\mathbf{s}^* = \{\tau_0^*, \boldsymbol{\tau}^*, \boldsymbol{\rho}^*, P^*\}$ as the optimal solution of the problem $\mathbf{P1}$. Now, we construct another transmission power of the HAP P' which satisfies $P_{\max} \geq P' > P^*$. Thus, the optimal ET duration is changed to $\tau_0' T = \frac{\tau_0^* T P^*}{P'} < \tau_0^* T$, which means there has residual time of $\tau_0^* T\big(1 - \frac{P^*}{P'}\big)$. Then, we allocate these time to all SNs such that $E_1^{a'} = E_2^{a'} = \cdots = E_N^{a'}$. We denote this solution as $\mathbf{s}' = \big\{\tau_0', \boldsymbol{\tau}', \boldsymbol{\rho}^*, P'\big\}$. Comparing to the solution $\mathbf{s}^*$, each SN's duration of IT phase in solution $\mathbf{s}'$ is longer. Thus, according to **Lemma 1**, the energy supply demand for the HAP of each SN in solution $\mathbf{s}'$ is smaller than that in solution $\mathbf{s}^*$, i.e., $E_1^{a'} = E_2^{a'} = \cdots = E_N^{a'} < \tau_0^* T P^*$. Finally, based on $\mathbf{s}'$, we change the duration of ET phase as $\tau_0'' = \frac{E_1^{a'}}{TP'}$. Thus, a new feasible solution can be expressed as $\mathbf{s}'' = \big\{\tau_0'', \boldsymbol{\tau}', \boldsymbol{\rho}^*, P'\big\}$. It is easy to verify that the solution $\mathbf{s}''$ satisfies all constraints of problem $\mathbf{P1}$. In addition, the solution $\mathbf{s}''$ consumes less energy than that of the solution $\mathbf{s}^*$, which indicates that the solution $\mathbf{s}^*$ is not the optimal solution. This contradicts with the assumption. The proof completes. □

By substituting the optimal PS factor ρ_i^* and the optimal transmission power of the HAP $P_{\max}$ into the ECM-TH problem $\mathbf{P1}$, we can obtain an equivalent optimization problem $\mathbf{P2}$ as follows:

$$\begin{aligned} \mathbf{P2}: &\min_{\tau_0, \boldsymbol{\tau}} \tau_0 \\ &s.t.\ C1: \tau_i TW \log_2\left(1 + \frac{\widehat{\theta}_i \tau_0}{\tau_i}\right) = D_i, \forall i \in \mathcal{N}_s \\ &\quad C3, C5, C6 \ \text{ in } \ \mathbf{P1} \end{aligned} \tag{25}$$

where $\widehat{\theta}_i = \widetilde{\theta}_i P_{\max}$.

It has been proved that $\tau_i TW \log_2\big(1 + \widehat{\theta}_i \tau_0/\tau_i\big)$ is a concave function of τ_0 and $\boldsymbol{\tau}$ for any given $i \in \mathcal{N}_s$ in Lemma 3.1 in [6]. Furthermore, constraints $C3$, $C5$ and $C6$ are all linear functions of τ_0 and τ_i. Thus, the ECM-TH problem $\mathbf{P2}$ is a convex optimization problem. Interior-point method [25] is one of the methods to solve both linear and nonlinear convex optimization problems by introducing barrier functions. However, the closed-form expression of solution is difficult to obtain by utilizing the interior-point method, and the computational complexity of the method is high since it iterates many times on updating primal and dual feasible solutions. Thus, we design a novel low-complexity hybrid method to solve the above optimization problem $\mathbf{P2}$ based on the GD and BS algorithms.

B. Optimization Approach

For a given τ_0, a closed-form solution of τ_i cannot be obtained directly by solving $C1$ in problem $\mathbf{P2}$. However, the solution of τ_i can be obtained iteratively by the fixed-point iteration, a method to obtain the solution of an equation by finite iterations. It has been proved in [13] that the solution of τ_i in $C1$ for a given τ_0 can be obtained by the following fixed-point iteration with linear convergence rate:

$$\tau_i(n+1) = \frac{D_i}{TW \log_2\left[1 + \frac{\widehat{\theta}_i \tau_0}{\tau_i(n)}\right]}, \forall i \in \mathcal{N}_s, \tag{26}$$

where n is the iteration index. In addition, we define

$$r(\tau_0) = \tau_0 + \sum_{i=1}^{N} \tau_i, \tag{27}$$

as the allocated sum ratios of one time slot T for a given τ_0.

Theorem 1. *$r(\tau_0)$ is a strictly convex function of τ_0.*

Proof. The constraint $C1$ in $\boldsymbol{P2}$ can be rewritten as

$$\tau_0 = \frac{\tau_i}{\widehat{\theta}_i}\Big(2^{\frac{M_i}{\tau_i}} - 1\Big), \tag{28}$$

where $M_i = D_i/(TW)$. By taking the derivative of both sides of (28), we can get

$$\mathrm{d}\tau_0 = \left(2^{\frac{M_i}{\tau_i}} \frac{\tau_i - M_i \ln 2}{\widehat{\theta}_i \tau_i} - \frac{1}{\widehat{\theta}_i}\right) \mathrm{d}\tau_i. \tag{29}$$

Thus, the derivative of τ_i with respect to τ_0 is expressed as

$$\frac{\mathrm{d}\tau_i}{\mathrm{d}\tau_0} = \frac{\widehat{\theta}_i \tau_i}{2^{\frac{M_i}{\tau_i}}(\tau_i - M_i \ln 2) - \tau_i}. \tag{30}$$

Let $X_i = 2^{\frac{M_i}{\tau_i}}(\tau_i - M_i \ln 2) - \tau_i$. Then, we can derive $\mathrm{d}^2\tau_i/\mathrm{d}\tau_0^2$ according to (30) as follows:

$$\begin{aligned} \frac{\mathrm{d}^2\tau_i}{\mathrm{d}\tau_0^2} &= \frac{\widehat{\theta}_i \frac{\mathrm{d}\tau_i}{\mathrm{d}\tau_0} X_i - \widehat{\theta}_i \tau_i \frac{\mathrm{d}X_i}{\mathrm{d}\tau_0}}{X_i^2} \\ &= \frac{\widehat{\theta}_i^2 \tau_i}{X_i^2} - \frac{\widehat{\theta}_i^2 \tau_i \cdot 2^{\frac{M_i}{\tau_i}}(\tau_i - \ln 2 \cdot M_i)}{X_i^3} \\ &\quad - \frac{\widehat{\theta}_i M_i (\ln 2)^2 \cdot 2^{\frac{M_i}{\tau_i}} \cdot M_i \widehat{\theta}_i}{X_i^3} + \frac{\widehat{\theta}_i^2 \tau_i^2}{X_i^3} \\ &= -\frac{\widehat{\theta}_i^2 M_i^2 (\ln 2)^2 \cdot 2^{\frac{M_i}{\tau_i}}}{X_i^3}. \end{aligned} \tag{31}$$

It has been proved in **Lemma 1** that E_i^a is a monotonically decreasing function with respect to τ_i. According to (23), $E_i^a = \tau_0 TP$ for any $i \in \mathcal{N}_s$. Moreover, T is a constant and $P^* = P_{\max}$ is also a constant according to **Lemma 2**. Thus, **Lemma 1** can be rephrased as τ_0 is a monotonically decreasing function with respect to τ_i, which means that τ_i will decrease with the increase of τ_0, i.e., $\mathrm{d}\tau_i/\mathrm{d}\tau_0 < 0$. Then, according to (30), since $\widehat{\theta}_i \tau_i$ is large than zero, we can obtain that $X_i < 0$. Thus, $\mathrm{d}^2\tau_i/\mathrm{d}\tau_0^2 > 0$ can be obtained according to (31), which indicates that τ_i is a strictly convex function with respect to τ_0. Since $r(\tau_0)$ is a linear combination of τ_0 and τ_i, $r(\tau_0)$ is also a strictly convex function of τ_0. The proof completes. □

As an example, one curve of $r(\tau_0)$ is given in Fig. 3. We take $N = 10$, $K = 4$ and $P_{\max} = 1$ mW. The distances

between SNs and the HAP are set varying from 0.35 to 0.8 meter with an interval of 0.05 meter. Throughput requirements of SNs are set randomly within $[1, 3]$ Mbps. It can be observed that $r(\tau_0)$ is indeed a convex function with respect to τ_0 which verifies the **Theorem 1**. We will obtain two solutions of τ_0 when we set $r(\tau_0) = 1$ in Fig. 3. The interval $[\tau_0^-, \tau_0^+]$ is the feasible set of τ_0. Obviously, the optimal solution of τ_0 in Fig. 3 is τ_0^- for the ECM-TH problem $\mathbf{P2}$.

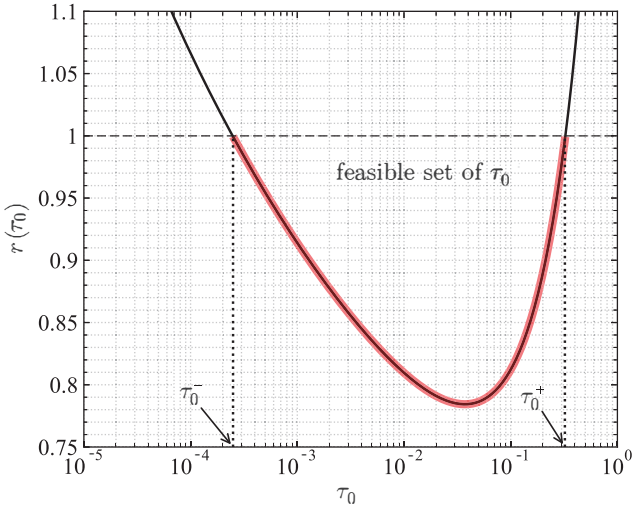

Fig. 3. One curve of $r(\tau_0)$, where $N = 10$, $K = 4$ and $P_{\max} = 1$ mW.

Below, under the situation that the optimal solutions of the problem $\mathbf{P2}$ exist, we design an efficient hybrid method to find the optimal solutions which is expressed as $\{\tau_0^*, \tau_1^*, \tau_2^*, \cdots, \tau_N^*\}$ based on the combining of the GD and BS algorithms. $r'(\tau_0)$ is denoted as the derivative of $r(\tau_0)$ with respect to τ_0. According to (27) and (30), $r'(\tau_0)$ can be calculated as follows:

$$r'(\tau_0) = 1 + \sum_{i=1}^{N} \frac{\widehat{\theta}_i \tau_i}{2^{\frac{M_i}{\tau_i}}(\tau_i - M_i \ln 2) - \tau_i}. \tag{32}$$

Firstly, according to **Theorem 1**, we can use the GD algorithm based on (32) to find a feasible solution of $\widehat{\tau_0}$ such that $r(\widehat{\tau_0}) < 1$. In detail, $\widehat{\tau_0}$ is initialized with $1/2$. The iterative formula for updating $\widehat{\tau_0}$ is given as follows:

$$\widehat{\tau_0}(n+1) = \widehat{\tau_0}(n) - \mu r'(\widehat{\tau_0}(n)), \tag{33}$$

where n is the iteration index and $\mu = 1/n$ is the step size. After one feasible $\widehat{\tau_0}$ is found, the optimal solution of τ_0 which satisfies $r(\tau_0^*) = 1$ is in the feasible set of $(0, \widehat{\tau_0})$. Then, the BS algorithm is utilized to find τ_0^* in the range of $(0, \widehat{\tau_0})$. In detail, the lower and upper bounds of τ_0 are initialized with $\tau_0^l = 0$ and $\tau_0^u = \widehat{\tau_0}$. τ_0 is then obtained by the following equation:

$$\tau_0 = \frac{\tau_0^l + \tau_0^u}{2}. \tag{34}$$

Then, $r(\tau_0)$ can be calculated by (26) and (27). If $r(\tau_0) > 1$, we set $\tau_0^l = \tau_0$, otherwise we set $\tau_0^u = \tau_0$. The value of τ_0^* can be obtained by repeating above steps of the BS algorithm until $\tau_0^u - \tau_0^l < \epsilon_1$, where ϵ_1 is a given precision. Finally, after τ_0^* is obtained based on the GD algorithm and BS algorithm, the optimal solutions of $\boldsymbol{\tau}^*$ can be obtained by the fixed-point iteration in (26). The proposed hybrid method for solving the ECM-TH problem in battery-free WP-BAN ends here.

C. In Case of Empty Feasible Set

The above proposed hybrid method is under the situation that the optimal solutions exist. However, according to (10) and (11), the problem may be infeasible because of the poor channel conditions, high throughput requirements, small channel bandwidth, low energy conversion efficiency, low transmission power of the HAP and large optimal PS factor.

Taking Fig. 3 as an example, there are two possible cases when there is no feasible solution:

- Case 1: $\min\{r(\tau_0)\} > 1, \forall\ \tau_0 \in [\tau_0^-, \tau_0^+]$.
- Case 2: $\max\{p_i(\tau_0^*, \tau_i^*)\} > p_{\max}, \forall\ i \in \mathcal{N}_s$.

Case 1 means that there is no solution to meet all SNs' throughput requirements within one time slot T. Case 2 means that there is no solution to meet all SNs' throughput requirements under the power limitation within one time slot T. Thus, when one of the above two cases occurs, there should be a corresponding scheme to handle it.

To simplify the following description, we first define a transmission priority weight w_i for the ith SNs. The value of weight is large or equal than zero. When the feasible set of the optimization problem is empty, we need to ignore some SNs' transmission requirement. The probability of ith SN being ignored can be calculated by

$$\pi_i = \frac{w_i}{\sum_{i=1}^{N} w_i}, \forall i \in \mathcal{N}_s, \tag{35}$$

which indicates that the greater the value of w_i, the greater the probability that the ith SN will be ignored. When the value of w_i is equal to zero, it means that the ith SN will never be ignored.

Before solving the ECM-TH problem by the hybrid method, we first determine whether Case 1 will happen. In detail, we use the GD algorithm based on (32) and (33) to find the minimum value of $r(\tau_0)$ iteratively. The iteration stops when $|r'(\tau_0)| < \epsilon_2$, where ϵ_2 is a given precision. In addition, once the value of $r(\tau_0)$ is less than 1, we also stop the iteration since it can be sure that the Case 1 will not occur. If the minimum value of $r(\tau_0)$ is greater than 1, i.e., $\min\{r(\tau_0)\} > 1$, the feasible set of the problem is empty. We will ignore the throughput requirement of one SN based on (35), i.e., set $\tau_i^* = 0$, and try to meet the throughput requirements of all the remaining SNs of $\mathcal{N}_s \backslash \{i\}$, where $\mathcal{N}_s \backslash \{i\}$ means the set $\mathcal{N}_s$ without SN i. The above steps are repeated until the feasible set is not empty. Then, τ_0^* and $\boldsymbol{\tau}^*$ can be calculated by the proposed hybrid method. Meanwhile, the values of $\boldsymbol{p}^*$ can be obtained by (8) based on τ_0^* and $\boldsymbol{\tau}^*$, where $\boldsymbol{p} = \{p_1, p_2, \cdots, p_N\}$. Now, we focus on the constraint $C3$. It has been proved in **Theorem 1** that $\mathrm{d}\tau_i/\mathrm{d}\tau_0 < 0$, i.e, τ_i will increase with the decrease of τ_0. Then, according to equation (8), we can conclude that p_i will decrease with the decrease of τ_0. It indicates that when the optimal solution τ_0^* is obtained, the transmission power of the SNs is the lowest among all feasible solutions. Thus, if $\max\{\boldsymbol{p}^*\} > p_{\max}$, i.e.,

the Case 2 occurs, it also means the feasible set is empty. We then ignore the throughput requirement of one SN chosen according to (35) and recalculate τ_0^*, $\boldsymbol{\tau}^*$ and $\boldsymbol{p}^*$ again until $\max\{\boldsymbol{p}^*\} \leq p_{\max}$.

The complete ECM-TH resource allocation scheme in battery-free WP-BAN is summarized as in **Algorithm 1**. Before each time slot starts, the values of the optimal PS factor $\boldsymbol{\rho}^*$ and the optimal time allocation τ_0^* and $\boldsymbol{\tau}^*$ are calculated in the HAP based on the **Algorithm 1**. And $\boldsymbol{\rho}^*$ is transmitted to SNs once it is calculated before IT phase.

Algorithm 1: Proposed Resource Allocation Scheme for ECM-TH in Battery-free WP-BAN

Initialize $P^* = P_{\max}$, $\widehat{\tau_0} = \frac{1}{2}$
calculate $\boldsymbol{\rho}^* = \{\rho_1^*, \rho_2^*, \cdots, \rho_N^*\}$ by (19)
// Corresponding steps for the empty feasible set:
repeat
  calculate $\boldsymbol{\tau}$ by (26) iteratively
  calculate $r'(\widehat{\tau_0})$ by (32)
  update $\widehat{\tau_0}$ by (33)
  calculate $r(\widehat{\tau_0})$ by $\widehat{\tau_0}$, (26) and (27)
  if $r(\widehat{\tau_0}) \leq 1$ **then**
    break;
until $|r'(\widehat{\tau_0})| < \epsilon_2$;
if $r(\widehat{\tau_0}) > 1$ **then**
  choose $i \in \mathcal{N}_s$ based on (35)
  set $\tau_i^* = 0$ and $\rho_i^* = 0$
  $\mathcal{N}_s = \mathcal{N}_s \backslash \{i\}$
  if $\mathcal{N}_s$ *is null* **then**
    set $\tau_0^* = 0$, $\boldsymbol{\tau}^* = 0$, go to step 33
  else
    return to step 4
// Proposed hybrid method:
Set $\tau_0^l = 0, \tau_0^u = \widehat{\tau_0}$.
repeat
  calculate τ_0 by (34)
  calculate $r(\tau_0)$ by τ_0, (26) and (27)
  if $r(\tau_0) > 1$ **then**
    $\tau_0^l = \tau_0$
  else
    $\tau_0^u = \tau_0$
until $\tau_0^u - \tau_0^l < \epsilon_1$;
calculate τ_0^*, $\boldsymbol{\tau}^*$ and $\boldsymbol{p}^*$ by (34), (26) and (8)
if $\max\{\boldsymbol{p}^*\} > p_{\max}$ **then**
  return to step 13
return the optimal time allocation τ_0^*, $\boldsymbol{\tau}^*$

IV. ECM-TH Problem in battery-assisted WP-BANs

In Section III, when the feasible set of the resource allocation optimization problem is empty, some SNs will not transmit sensory data to the HAP. We define the outage probability as the ratio of the number of times when the SNs fail to achieve the throughput requirements to the total transmission times of SNs. In the battery-free WP-BAN, the outage probability is high when the channel conditions are poor or the throughput requirements of SNs are high. In order to decrease the outage probability, we investigate ECM-TH problem in the battery-assisted WP-BAN in this section.

A. Problem Formulation

According to the analysis in Section II, during each time slot of the battery-assisted scenario, the HAP consumes $\tau_0 TP$ amount of energy, the SNs harvest $\sum_{i=1}^{N} E_i$ amount of energy and consume $\frac{1}{\alpha}\sum_{i=1}^{N}\tau_i T p_i$ amount of energy on IT and the circuit. Thus, the ECM-TH problem in battery-assisted WP-BAN can be formulated as follows

$$\begin{aligned}
\mathbf{P3}: \min_{\tau_0,\boldsymbol{\tau},\boldsymbol{\rho},\boldsymbol{p},P} \ & \tau_0 TP - \sum_{i=1}^{N} E_i + \frac{1}{\alpha}\sum_{i=1}^{N}\tau_i T p_i \\
s.t.\ & C1': \tau_i TW\log_2\left(1+\frac{p_i\left|\left|\mathbf{g}_i\right|\right|^2}{\sigma_a^2}\right) \geq D_i, \forall i \in \mathcal{N}_s \\
& C7: \frac{1}{\alpha}\tau_i T p_i \leq B_i + E_i,\ \forall i \in \mathcal{N}_s \\
& C8: B_i + E_i \leq B_{\max},\ \forall i \in \mathcal{N}_s \\
& C2 - C6 \ \text{ in } \ \mathbf{P1}
\end{aligned} \tag{36}$$

where $C7$ and $C8$ are constraints on energy causality and on preventing energy overflow.

Based on the analysis in Section III, the optimal PS factor of the ith SN ρ_i^* can be obtained by (19) under the constraint $C2$. Moreover, as in the battery-free scenario, we should only transmit the required amount of the throughput in order to decrease energy consumption. Thus, the inequality in constraint $C1'$ becomes equality in problem $\mathbf{P3}$, i.e., $C1'$ is transformed to

$$\tau_i TW\log_2\left(1+\frac{p_i\left|\left|\mathbf{g}_i\right|\right|^2}{\sigma_a^2}\right) = D_i, \forall i \in \mathcal{N}_s. \tag{37}$$

By rearranging (37), we can get the following equation:

$$\tau_i T p_i = \frac{\sigma_a^2 \tau_i T}{\left|\left|\mathbf{g}_i\right|\right|^2}\left(2^{\frac{D_i}{\tau_i TW}} - 1\right), \forall i \in \mathcal{N}_s. \tag{38}$$

We define $E_i^s \triangleq \tau_i T p_i$, which represents the amount of consumed energy of the ith SN on IT.

Lemma 3. *E_i^s is a monotonically decreasing function with respect to τ_i under the constraint of $C1'$, where $0 \leq \tau_i \leq 1$.*

Proof. According to (38), the derivative of E_i^s with respect to τ_i is

$$\begin{aligned}
\frac{dE_i^s}{d\tau_i} &= \frac{\sigma_a^2 T}{\left|\left|\mathbf{g}_i\right|\right|^2}\left(2^{\frac{D_i}{\tau_i TW}} - 1 - 2^{\frac{D_i}{\tau_i TW}}\cdot\frac{D_i}{\tau_i TW}\cdot\ln 2\right) \\
&= \frac{\sigma_a^2 T}{\left|\left|\mathbf{g}_i\right|\right|^2}\left(x_i - x_i \ln x_i - 1\right),
\end{aligned} \tag{39}$$

where $x_i = 2^{\frac{D_i}{\tau_i TW}}$ which is greater than 1. Since the inequality $x_i - x_i\ln x_i - 1 < 0$ holds for any $x_i > 1$, we have $dE_i^s/d\tau_i < 0$. Thus, E_i^s is a monotonically decreasing function with respective to τ_i. The proof completes. □

Lemma 4. *The optimal transmission power of the HAP P^* in ECM-TH problem* $\mathbf{P3}$ *is equal to* $P_{\max}$ *when* $\tau_0 \neq 0$.

Proof. We prove it by contradiction. Assume there is an optimal transmission power of the HAP $P^* < P_{\max}$. We denote $\mathbf{s}^* = \{\tau_0^*, \boldsymbol{\tau}^*, \boldsymbol{\rho}^*, \boldsymbol{p}^*, P^*\}$ as the optimal solution of the problem $\mathbf{P3}$. Now, we construct another transmission power of the HAP P' where $P_{\max} \geq P' > P^*$. Moreover, we construct $\tau_0' = \frac{P^*}{P'}\tau_0^* < \tau_0^*$ which guarantees that $\tau_0' P' = \tau_0^* P^*$. Thus, there has residual time of $\tau_0^* T\big(1 - \frac{P^*}{P'}\big)$. Then, we allocate these time to all SNs in the duration of IT. We denote this solution as $\mathbf{s}' = \{\tau_0', \boldsymbol{\tau}', \boldsymbol{\rho}^*, \boldsymbol{p}', P'\}$. Then, according to **Lemma 3**, $E_i^s = \tau_i T p_i$ decreases with the increasing of τ_i. In addition, $\tau_0' P' = \tau_0^* P^*$. Therefore, the value of the objective function in $\mathbf{P3}$ under the solution $\mathbf{s}'$ is less than that under the solution $\mathbf{s}^*$, which indicates that the solution $\mathbf{s}^*$ is not the optimal solution. This contradicts with the assumption. The proof completes. □

By substituting the optimal PS factor vector $\boldsymbol{\rho}^*$ and the optimal transmission power of the HAP $P_{\max}$ into the ECM-TH problem $\mathbf{P3}$, a new optimization problem $\mathbf{P4}$ is obtained as follows:

$$\begin{aligned} \mathbf{P4}: &\min_{\tau_0, \boldsymbol{\tau}, \boldsymbol{p}} \tau_0 T P_{\max}(1 - \sum_{i=1}^{N} \Theta_i) + \frac{1}{\alpha}\sum_{i=1}^{N} \tau_i T p_i \\ &s.t.\ C1', C3, C5 - C8 \ \text{ in } \ \mathbf{P3} \end{aligned} \tag{40}$$

where $\Theta_i = \eta(1 - \rho_i^*)\sum_{j=1}^{N} |\mathbf{h}_i \mathbf{w}_j|^2$. Since the objective function, constraints $C1'$, $C7$ and $C8$ include products of optimization variables, the optimization problem $\mathbf{P4}$ is non-convex. In order to transform it into a convex problem, we introduce auxiliary variables $V_i = \tau_i p_i$ into problem $\mathbf{P4}$. Then the problem $\mathbf{P4}$ is transformed to the following equivalent problem:

$$\begin{aligned} \mathbf{P5}: &\min_{\tau_0, \boldsymbol{\tau}, \boldsymbol{V}} \tau_0 T P_{\max}(1 - \sum_{i=1}^{N} \Theta_i) + \frac{T}{\alpha}\sum_{i=1}^{N} V_i \\ &s.t.\ C1': \tau_i T W \log_2\left(1 + \frac{V_i ||\mathbf{g}_i||^2}{\tau_i \sigma_a^2}\right) \geq D_i, \forall i \in \mathcal{N}_s \\ &\quad C3: 0 \leq V_i \leq \tau_i p_{\max},\ \forall i \in \mathcal{N}_s \\ &\quad C7: V_i T \leq (B_i + E_i)\alpha,\ \forall i \in \mathcal{N}_s \\ &\quad C5, C6, C8 \ \text{ in } \ \mathbf{P3} \end{aligned} \tag{41}$$

where $\boldsymbol{V} = \{V_1, V_2, \cdots, V_N\}$.

B. Optimization Approach

It can be observed that constraint $C1'$ has the similar expression form as the constraint $C1$ in problem $\mathbf{P2}$. Therefore, the constraint $C1'$ is also a concave function with respect to $\boldsymbol{\tau}$ and $\boldsymbol{V}$. In addition, the objective function and the other constraints in problem $\mathbf{P5}$ are all linear function with respect to the variables to be optimized. Therefore, the problem $\mathbf{P5}$ is a standard convex optimization problem of τ_0, $\boldsymbol{\tau}$ and $\boldsymbol{V}$. We solve the problem $\mathbf{P5}$ by Lagrange dual subgradient method which combines Lagrange dual method and subgradient method. The Lagrangian function of the problem $\mathbf{P5}$ is

$$\begin{aligned} \mathcal{L} =& \tau_0 T P_{\max}\left(1 - \sum_{i=1}^{N}\Theta_i\right) + \frac{T}{\alpha}\sum_{i=1}^{N} V_i \\ &+ \sum_{i=1}^{N}\lambda_i\left[D_i - \tau_i T W \log_2\left(1 + \frac{V_i ||\mathbf{g}_i||^2}{\tau_i \sigma_a^2}\right)\right] \\ &+ \sum_{i=1}^{N}\alpha_i\left(V_i - \tau_i p_{\max}\right) + \sum_{i=1}^{N}\mu_i\left[V_i T - (B_i + E_i)\alpha\right] \\ &+ \sum_{i=1}^{N}\beta_i\left(B_i + E_i - B_{\max}\right) + \varsigma\left(\sum_{i=0}^{N}\tau_i - 1\right), \end{aligned} \tag{42}$$

where $\boldsymbol{\lambda} = \{\lambda_1, \lambda_2, \cdots, \lambda_N\}$, $\boldsymbol{\alpha} = \{\alpha_1, \alpha_2, \cdots, \alpha_N\}$, ς, $\boldsymbol{\mu} = \{\mu_1, \mu_2, \cdots, \mu_N\}$ and $\boldsymbol{\beta} = \{\beta_1, \beta_2, \cdots, \beta_N\}$ are Lagrange multipliers of constraints $C1'$, $C3$, $C5$, $C7$ and $C8$, respectively. Then, the derivative of Lagrangian function $\mathcal{L}$ with respect to V_i is

$$\frac{\partial \mathcal{L}}{\partial V_i} = \frac{T}{\alpha} - \frac{1}{\ln 2}\frac{\lambda_i \tau_i T W}{1 + \frac{V_i ||\mathbf{g}_i||^2}{\tau_i \sigma_a^2}} \cdot \frac{||\mathbf{g}_i||^2}{\tau_i \sigma_a^2} + \alpha_i + \mu_i T,\ \forall i \in \mathcal{N}_s. \tag{43}$$

By setting (43) to zero, we can get the value of p_i when $\mathcal{L}$ is minimized, i.e.,

$$p_i = \frac{V_i}{\tau_i} = \left[\frac{\lambda_i T W}{\left(\frac{T}{\alpha} + \alpha_i + \mu_i T\right)\ln 2} - \frac{\sigma_a^2}{||\mathbf{g}_i||^2}\right]_0^{p_{\max}}, \forall i \in \mathcal{N}_s, \tag{44}$$

where $[\cdot]_a^b$ denotes $\min\{\max\{\cdot, a\}, b\}$. The derivative of Lagrangian function $\mathcal{L}$ with respect to τ_0 is

$$\frac{\partial \mathcal{L}}{\partial \tau_0} = T P_{\max}\left[1 - \sum_{i=1}^{N}\Theta_i\left(1 + \mu_i - \beta_i\right)\right]. \tag{45}$$

By replacing V_i with $\tau_i p_i$, the derivative of Lagrangian function $\mathcal{L}$ with respect to τ_i can be obtained as follows:

$$\begin{aligned} \frac{\partial \mathcal{L}}{\partial \tau_i} =& p_i T\left(\frac{1}{\alpha} + \mu_i\right) + \alpha_i(p_i - p_{\max}) + \varsigma \\ &- \lambda_i T W \log_2\left(1 + p_i \frac{||\mathbf{g}_i||^2}{\sigma_a^2}\right),\ \forall i \in \mathcal{N}_s, \end{aligned} \tag{46}$$

where the value of p_i can be calculated by (44). Thus, according to (45) and (46), we find that the Lagrangian function $\mathcal{L}$ is a linear function of both τ_0 and τ_i, which means that the optimal solutions of τ_0 and $\boldsymbol{\tau}$ can always be found for a given p_i at the vertices of the feasible region.

Therefore, for a given p_i, the optimal solutions of τ_0 and $\boldsymbol{\tau}$ can be obtained by taking p_i into problem $\mathbf{P4}$, the problem is then transformed to a linear programming of τ_0 and $\boldsymbol{\tau}$ which can be solved by linear optimization techniques. Finally, the value of V_i can be obtained by taking τ_i and p_i into (44). Thus, for any given λ_i, α_i and μ_i, we can obtain τ_0, $\boldsymbol{\tau}$ and $\boldsymbol{V}$ through above steps. The Lagrange multipliers λ_i, α_i, μ_i,

β_i and ς can be updated based on the values of τ_0, $\boldsymbol{\tau}$ and $\boldsymbol{V}$ through the subgradient method by the following equations:

$$\begin{cases} \lambda_i(n+1) = [\lambda_i(n) + \Delta_n(D_i - R_i)]^+, \forall i \in \mathcal{N}_s \\ \alpha_i(n+1) = [\alpha_i(n) + \Delta_n(V_i - \tau_i p_{\max})]^+, \forall i \in \mathcal{N}_s \\ \mu_i(n+1) = [\mu_i(n) + \Delta_n(V_i T - \alpha B_i - \alpha E_i)]^+, \forall i \in \mathcal{N}_s \\ \beta_i(n+1) = [\beta_i(n) + \Delta_n(B_i + E_i - B_{\max})]^+, \forall i \in \mathcal{N}_s \\ \varsigma(n+1) = \left[\varsigma(n) + \Delta_n(\sum_{i=0}^{N} \tau_i - 1)\right]^+ \end{cases} \tag{47}$$

where $[\cdot]^+$ denotes $\max\{\cdot, 0\}$. n is the iteration index. Δ_n is the step size of the nth iteration which satisfies

$$\Delta_n > 0, \lim_{n \to +\infty} \Delta_n = 0, \lim_{n \to +\infty} \sum_{i=1}^{n} \Delta_n = +\infty. \tag{48}$$

We denote x as one element of the set $\{\boldsymbol{\lambda}, \boldsymbol{\alpha}, \boldsymbol{\mu}, \boldsymbol{\beta}, \varsigma\}$. When all of the Lagrange multipliers converge, i.e.,

$$|x(n+1) - x(n)| \leq \epsilon_3, \ \forall x \in \{\boldsymbol{\lambda}, \boldsymbol{\alpha}, \boldsymbol{\mu}, \boldsymbol{\beta}, \varsigma\}, \tag{49}$$

the optimal transmission power of SNs can be calculated by (44), and the optimal time allocations of the ET and IT can be obtained by taking $\boldsymbol{p}^*$ into the problem $\mathbf{P4}$. ϵ_3 in (49) is a given error precision. Since the convexity of the problem $\mathbf{P5}$, the iterative optimization between the primal variables and the dual variables is guaranteed to converge to the optimal solutions of $\mathbf{P5}$ [25]. In detail, according to (47) and (48), Lagrange multipliers are equal to zero when the relevant constraints do not work. Conversely, if the constraints work, the related Lagrangian multipliers will eventually converge to positive values.

C. In Case of Empty Feasible Set

Similar to Section III, the above algorithm for solving the ECM-TH problem in the battery-assisted WP-BAN is under the situation that the optimal solutions exist. In this subsection, the case when the feasible set is empty is addressed. We need to judge whether the feasible set is empty before solving the ECM-TH problem. We presume that each SN consumes all the harvested energy and the remaining energy in the battery at each time slot. Thus, the achievable throughput of the ith SN is transformed to

$$R_i = \tau_i T W \log_2\left(1 + \frac{\widehat{\theta}_i \tau_0}{\tau_i} + \frac{\alpha B_i ||\mathbf{g}_i||^2}{\sigma_a^2 \tau_i T}\right), \forall i \in \mathcal{N}_s. \tag{50}$$

Furthermore, for a given τ_0, the solutions of τ_i under the throughput requirements constraint are able to be obtained by the following fixed-point iteration:

$$\tau_i(n+1) = \frac{D_i}{TW\log_2\left[1 + \frac{\widehat{\theta}_i \tau_0}{\tau_i(n)} + \frac{\alpha B_i ||\mathbf{g}||^2}{\sigma_a^2 \tau_i(n) T}\right]}, \forall i \in \mathcal{N}_s. \tag{51}$$

In addition, we find that equation (32) still holds for the battery-assisted scenario. Thus, we first use GD algorithm based on (32), (33) and (51) to find the minimum $r(\tau_0)$ iteratively. Once $r(\tau_0) \leq 1$, we stop the iteration since the feasible set is not empty. If $\min\{r(\tau_0)\} > 1$, the feasible set is empty, and we ignore the throughput requirement of one SN based on (35) as in Section III. The above steps are repeated until $\min\{r(\tau_0)\} \leq 1$. After the non-empty feasible set is obtained, the Lagrange dual subgradient method is utilized to solve the problem. The complete resource allocation scheme for solving the ECM-TH problem in battery-assisted WP-BAN is summarized in **Algorithm 2**. Before each time slot starts, the optimal resource allocation results are calculated in the HAP based on the **Algorithm 2**. And the optimal PS factor $\boldsymbol{\rho}^*$ is transmitted to SNs once it is calculated before IT phase.

Algorithm 2: Proposed Resource Allocation Scheme for ECM-TH in Battery-assisted WP-BAN

Initialize $\widehat{\tau_0} = \frac{1}{2}$ and Lagrange multipliers
calculate $\boldsymbol{\rho}^* = \{\rho_1^*, \rho_2^*, \cdots, \rho_N^*\}$ by (19)
// Corresponding steps for the empty feasible set:
repeat
  calculate $\boldsymbol{\tau}$ by (51) iteratively
  calculate $r'(\widehat{\tau_0})$ by (32)
  update $\widehat{\tau_0}$ by (33)
  calculate $r(\widehat{\tau_0})$ by $\widehat{\tau_0}$, (27) and (51)
  if $r(\widehat{\tau_0}) \leq 1$ **then**
    break;
until $|r'(\widehat{\tau_0})| < \epsilon_2$;
if $r(\widehat{\tau_0}) > 1$ **then**
  choose $i \in \mathcal{N}_s$ based on (35)
  set $\tau_i^* = 0$, $p_i^* = 0$ and $\rho_i^* = 0$
  $\mathcal{N}_s = \mathcal{N}_s \backslash \{i\}$
  if $\mathcal{N}_s$ *is null* **then**
    set $\tau_0^* = 0$, $\boldsymbol{\tau}^* = 0$, $\boldsymbol{p}^* = 0$, go to step 29
  else
    return to step 4
// Proposed Lagrange dual subgradient method:
repeat
  calculate $\boldsymbol{p}$ by (44)
  calculate τ_0 and $\boldsymbol{\tau}$ by taking $\boldsymbol{p}$ into the problem $\mathbf{P4}$ through linear programming techniques
  update $\boldsymbol{\lambda}$, $\boldsymbol{\alpha}$, $\boldsymbol{\mu}$, $\boldsymbol{\beta}$ and ς by (47)
until equation (49) holds;
calculate $\boldsymbol{p}^*$ by (44)
calculate τ_0^* and $\boldsymbol{\tau}^*$ by taking $\boldsymbol{p}^*$ into the problem $\mathbf{P4}$
update B_i by (13)
return the optimal time and power allocation τ_0^*, $\boldsymbol{\tau}^*$, $\boldsymbol{p}^*$

V. Simulation Results

In this section, we numerically study the performance of our proposed resource allocation schemes for solving the ECM-TH problem in both battery-free and battery-assisted WP-BAN. All the simulations are executed on a computer with an Intel Core i5 2.50-GHz CPU and 8 GB of memory. Corresponding parameters for all simulations are given as follows unless otherwise specified. The number of SNs and HAP's antennas is set to $N = 10$ and $K = 4$. We consider all SNs have a equally transmission priority, thus transmission priority weights of all SNs are set to 1. Since SNs in a WP-BAN are worn or even implanted in the human body, the

communication links between SNs and the HAP are interfered by cloths and human postures. Therefore, to depict the channel more realistically, the channel power gain of the WP-BAN is modeled as $|h_{i,j}|^2 = 10^{-\frac{L(d_0)+\psi_{i,j}}{10}} d_i^{-\delta} \xi_{i,j}$ [9], where $L(d_0) = 30$ dB is path loss at the reference distance d_0. $\delta = 3.8$ is the path loss exponent. d_i is the distance between the ith SN and the HAP. $\psi_{i,j}$ is a Gauss-distributed random variable with zero mean and variance of 15 dB, which denotes the body shadowing loss margin. $\xi_{i,j}$ denotes the small-scale fading that is modeled as Rayleigh fading with unit mean [31]. Time slot T, channel bandwidth W and SNR threshold γ_0 are set to 1 second, 1 MHz and 10 dB, respectively. Both energy conversion efficiency η and proportion of energy used for communication α are set to 0.8. The body temperature is set to 37 Celsius (T_0 = 310 kelvin). Noise figure F_i is set to 13 dB [11]. The variances of AWGN introduced by RF to baseband conversion δ_i^2 and by the receiving antenna at the HAP σ_a^2 are respectively set to -52 dBm and -114 dBm [31]. The error precision ϵ_1, ϵ_2 and ϵ_3 are both set to 10^{-9} seconds.

Fig. 4 displays the achievable throughput of each SN over one time slot T by the proposed resource allocation schemes for the ECM-TH problem. The STM [6], CTM [6] and SUM [9] schemes are used here for reference. $P_{\max}$ is fixed at 5 mW. For the purpose of showing the differences of the four schemes easily, only three SNs are adopted for this simulation. The distances between the HAP and SNs are set to $\{0.4, 0.6, 0.8\}$ meters. The dashed lines indicate the throughput requirements of each SN. Simulation result shows that the proposed schemes for ECM-TH in this paper meets the throughput requirements of all three SNs under the condition of throughput heterogeneity. For the STM scheme, the achievable throughput of SNs is extremely unbalance resulting in unreachable throughput for SN2 and SN3. For the CTM scheme, the throughput requirement of SN2 cannot be met. It is more suitable for the scenarios where all SNs have the same throughput requirement. The SUM scheme is a compromise between the STM scheme and the CTM scheme. However, the achievable throughput of SN2 is still lower than its requirement as shown in Fig. 4. The energy consumption comparison of the HAP over one time slot T between our proposed resource allocation schemes and the reference schemes in Fig. 4 are shown in Table III. Since the difference in objective of the STM, CTM, SUM schemes, the energy consumption of these three schemes is much higher than that of the proposed schemes. Moreover, it can be observed that the energy consumption in battery-assisted scenario is less than that in battery-free scenario. The reason is that in battery-free scenario, only time allocation is employed to solve the ECM-TH problem, whereas in battery-assisted scenario, joint time and power allocation is employed. In a battery-free scenario, the energy of SNs is wasted when the SNs fail to meet the throughput requirements, whereas in a battery-assisted scenario, their energy can be stored into a battery for future use by employing the proposed resource allocation scheme. However, the energy consumption of the STM, CTM and SUM schemes is the same in both two scenarios. The reason is that for these three schemes, SNs will also consume all the harvested energy to transmit sensory data in battery-assisted scenario.

TABLE III
ENERGY CONSUMPTION OF THE HAP OVER ONE TIME SLOT T

	In battery-free scenario (J)	In battery-assisted scenario (J)
Proposed	3.459×10^{-8}	4.375×10^{-9}
STM [6]	2.423×10^{-4}	2.423×10^{-4}
CTM [6]	6.074×10^{-4}	6.074×10^{-4}
SUM [9]	2.685×10^{-4}	2.685×10^{-4}

Fig. 5 demonstrates energy consumption of the proposed hybrid method and the interior-point method for ECM-TH versus the values of P under different γ_0. The throughput requirements of 10 SNs are set to $\{10.0, 5.0, 2.5, 1.536, 1.0, 0.864, 0.32, 0.192, 0.1, 0.001\}$Mbps, which is ranging from 1 kbps to 10 Mbps [3]. The distances between the HAP and SNs are set varying from 0.35 meter to 0.8 meter with an interval of 0.05 meter. The result shows that curves of the proposed hybrid method and the interior-point method coincide under the same value of γ_0,

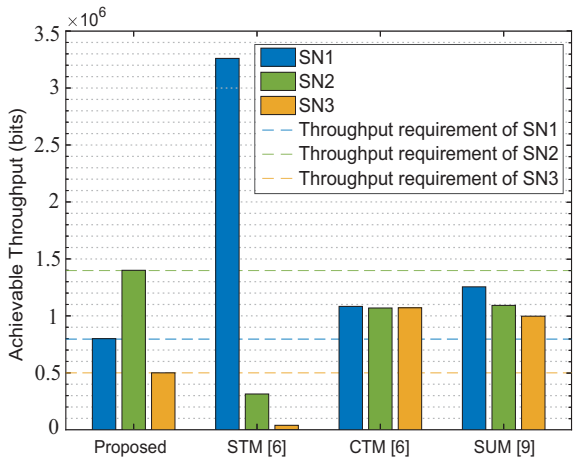

Fig. 4. Achievable throughput of each SN over one time slot T by the proposed resource allocation schemes for ECM-TH.

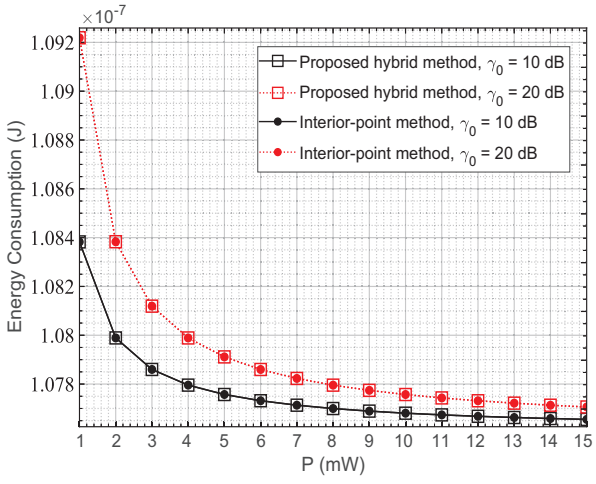

Fig. 5. The energy consumption of the proposed hybrid method and the interior-point method versus the value of P.

which indicates that the solutions of the hybrid method are the same as those of the interior-point method. Thus, the optimality of the proposed hybrid method is verified since the interior-point method can obtain the optimal solution to the convex optimization problem. It can be seen that energy consumption decreases with the increasing of P, which verifies the correctness of **Lemma 2** i.e. $P^* = P_{\max}$ in the battery-free scenario. We find that energy consumption increases with the increasing of γ_0, which can be explained by (19), i.e. SNs consume more energy on ID and less energy on IT when γ_0 increases.

Fig. 6 shows the computational complexity comparison between the proposed hybrid method and the interior-point method. Since the iterative formulas of these methods are different, we employ average running time over one time slot as the metric of the computational complexity. In order to make a fair comparison, two algorithms run on the same computer and under the same system parameters. The result shows that the proposed hybrid method takes much less time compared with the interior-point method and the gap becomes larger along with the increasing number of SNs. The reason is that the interior-point method iterates hundreds of times on updating primal and dual feasible solutions during each time slot which is unnecessary in the proposed method. Thus, our proposed hybrid method can achieve the same energy consumption performance as the interior-point method but with a lower computational complexity.

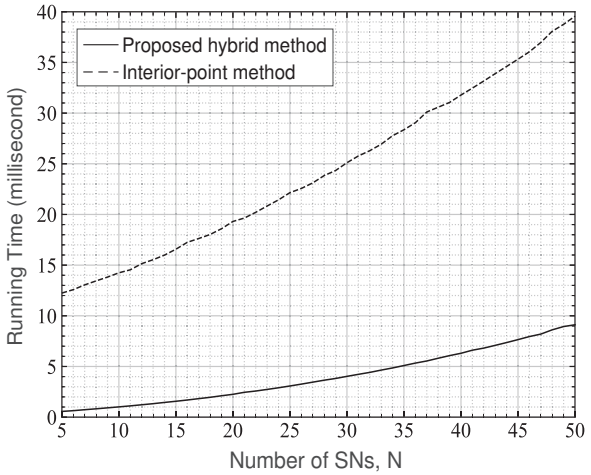

Fig. 6. Average running time comparison between the proposed hybrid method and the interior-point method over one time slot.

Fig. 7 compares the outage probability of SNs between battery-free and battery-assisted scenarios with different initial energy B_0 under different values of P. 20 SNs are deployed randomly around the HAP within the range [0.3, 1.0] meter. And the throughput requirements of these SNs are set randomly within the range [0, 2.5] Mbps. The simulation result shows that both the outage probabilities of the battery-free and battery-assisted scenarios decrease with the increasing of P. The reason is that the SNs are able to harvest more energy when the transmission power of the HAP is higher. It can be observed that compared with the battery-free scenario, the battery-assisted scenario achieves lower outage probability. This is because when a SN fails to meet the throughput requirements, its energy is wasted in a battery-free WP-BAN, whereas in a battery-assisted WP-BAN, its energy is stored into battery for future use based on the proposed resource allocation scheme. Moreover, SNs with more initial energy can lower the outage probability further. The reason is that an SN with more initial energy is able to decrease the rate of failure transmission for longer time.

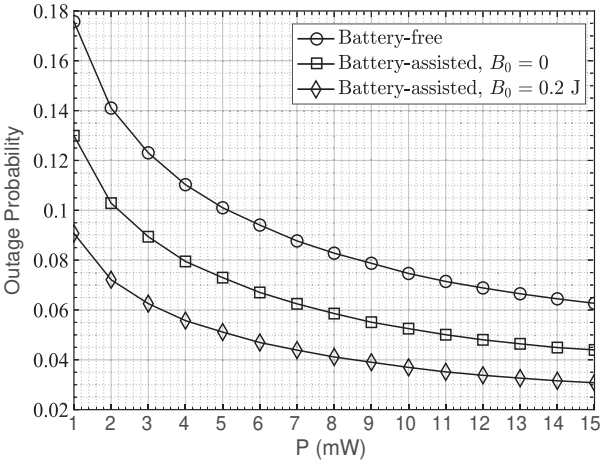

Fig. 7. The outage probability of the battery-free and battery-assisted scenarios under different values of P.

Fig. 8 illustrates the impact of throughput requirements of 20 SNs on the outage probability. The maximum transmission power $P_{\max}$ of the HAP is fixed at 10 mW. The throughput requirements of SNs are set randomly within the set [0, $D_{\max}$] Mbps during each time slot. The initial energy is zero in the battery-assisted scenario for a fair comparison. It shows that the outage probabilities of both battery-free and battery-assisted WP-BAN increase with the increasing of $D_{\max}$. The reason is that the average throughput requirements increase with the increasing of the $D_{\max}$ which results in the increasing of the energy consumption of SNs. Also, the outage

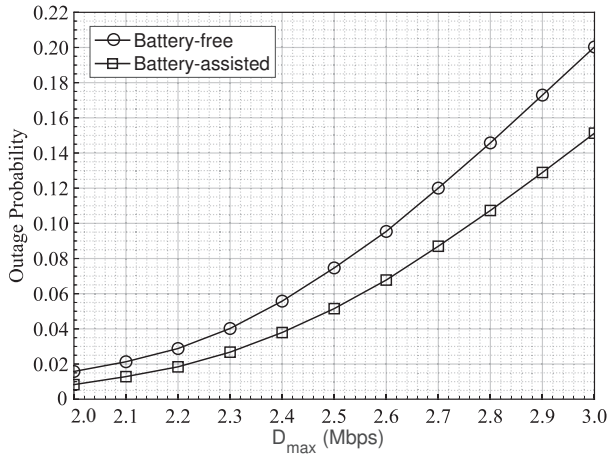

Fig. 8. The outage probability of the battery-free and battery-assisted scenarios under different values of $D_{\max}$.

probability of the battery-assisted WP-BAN is lower than that of the battery-free WP-BAN under the same throughput requirements.

Fig. 9 depicts energy consumption of the battery-free and battery-assisted scenarios under different number of SNs. The maximum transmission power of the HAP $P_{\max}$ is set to 10 mW. The distances between the HAP and SNs are fixed at 0.6 meter. In order to explore the impact of different throughput requirements of SNs on energy consumption, we set the throughput requirements within the ranges [0, 0.4] Mbps, [0.4, 0.8] Mbps and [0.8, 1.2] Mbps, respectively. The simulation results show that the energy consumption increases with the increasing number of SNs. The reason is that the total throughput requirements increase when the number of SNs increases, which results in the increasing of energy consumption of the system. Moreover, it can be observed that the larger throughput the SNs require, the faster the energy consumption of the system increases, which can be explained by (21). Under the same throughput requirements range, the battery-assisted SNs consume less energy than the battery-free SNs, and with the increasing number of SNs, the difference becomes bigger in this logarithmic scale. The reason is that the ratio of the energy lost during the ET phase to the energy consumption of the circuit and communication in the IT phase becomes larger when N increases. Please notice that in this figure we don't add any reference curve of other resource allocation scheme for comparison. The reason is that to the best of our knowledge, there is no study that investigates the ECM-TH problem in a WP-BAN. Also, the throughput heterogeneity cannot be achieved by other simple schemes e.g. equal or random allocation scheme.

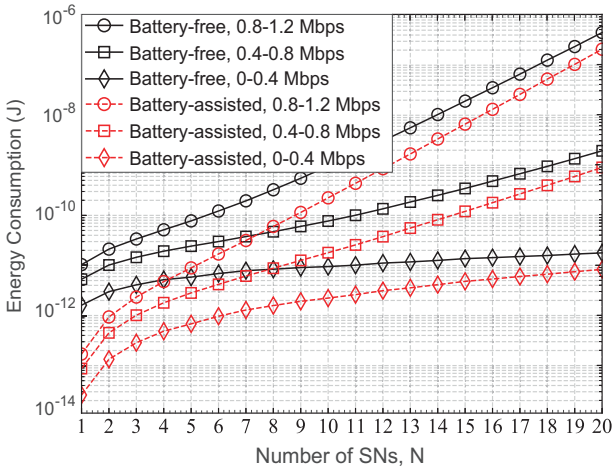

Fig. 9. The energy consumption of the battery-free and battery-assisted scenarios versus the number of SNs under different throughput requirements.

Fig. 10 demonstrates how the degree of the throughput heterogeneity and the allocation of SNs affect the energy consumption of WP-BAN. We use $U(a,b)$ to denote the uniform distribution on the interval $[a,b]$, with mean value of $\frac{a+b}{2}$ and variance of $\frac{(b-a)^2}{12}$. In the simulation, we set $D_i \sim U(\overline{D} - \sqrt{3\sigma_D^2}, \overline{D}+\sqrt{3\sigma_D^2})$ and $d_i \sim U(\overline{d}-\sqrt{3\sigma_d^2}, \overline{d}+\sqrt{3\sigma_d^2})$, where $\overline{D}$ and $\overline{d}$ denote the mean values of throughput requirements and of distances between SNs and the HAP. σ_D^2 and σ_d^2 denote the variances of throughput requirements and of distances between SNs and the HAP. The value of $\overline{D}$ and $\overline{d}$ are fixed at 1.5 Mbps and 0.6 meter. The variances are utilized to depict the heterogeneity degree. The simulation results show that the system energy consumption increases with the increasing of the degree of the throughput heterogeneity. For example, compared with the situation when $\sigma_D^2 = 0$, i.e. the same throughput requirements for all SNs, the energy consumption is about three or four times higher when $\sigma_D^2 = 0.5$ with the same average throughput $\overline{D}$. In order to explore the effect of SNs' allocation on system energy consumption, we set σ_d^2 to 0, 0.01 and 0.02 respectively. The results show that the more distributed of SNs, the more energy consumption required for WP-BAN, which can provide the guidance for the deployment of SNs.

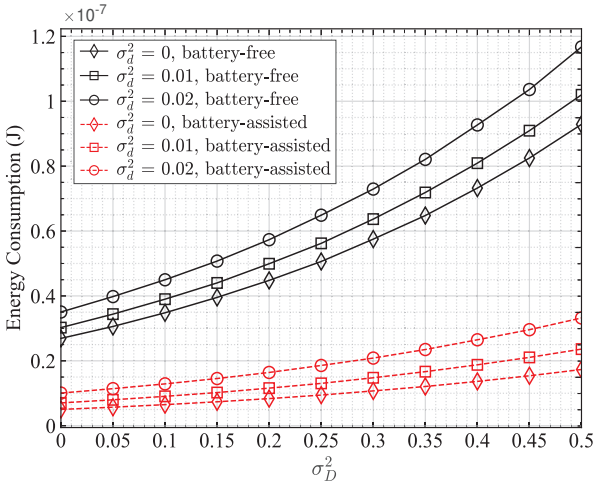

Fig. 10. The effect of the degree of the throughput heterogeneity and the allocation of SNs.

VI. Conclusion

Two resource allocation schemes for solving the ECM-TH problems in battery-free and battery-assisted WP-BANs have been proposed herein, respectively. For the battery-free scenario, a novel hybrid method of GD and BS is proposed that can achieve the same performance as the interior-point method with a lower computational complexity. For the battery-assisted scenario, the non-convex ECM-TH problem is first transformed into a convex problem and then solved using the Lagrange dual subgradient method. Compared with the battery-free scenario, both energy consumption and outage probability are lower in the battery-assisted scenario. Moreover, the cases of the empty feasible set in the ECM-TH problems are considered and addressed in both scenarios.

References

[1] L. Chettri and R. Bera, "A comprehensive survey on internet of things (IoT) toward 5G wireless systems," *IEEE Internet Things J.*, vol. 7, no. 1, pp. 16-32, Jan. 2020.

[2] L. D. Xu, W. He, and S. Li, "Internet of things in industries: A survey," *IEEE Trans. Ind. Informat.*, vol. 10, no. 4, pp. 2233-2243, Nov. 2014.

[3] M. Salayma, A. Al-Dubai, I. Romdhani and Y. Nasser, "Wireless body area network (WBAN): A survey on reliability, fault tolerance, and technologies coexistence," *ACM Comput. Surveys*, vol. 50, no. 1, pp. 1-38, Mar. 2017.

[4] Y. Alsaba, S. K. A. Rahim, and C. Y. Leow, "Beamforming in wireless energy harvesting communications systems: A survey," *IEEE Commun. Surveys Tuts.*, vol. 20, no. 2, pp. 1329-1360, Jan. 2018.

[5] T. D. P. Perera, D. N. K. Jayakody, S. K. Sharma, S. Chatzinotas, and J. Li, "Simultaneous wireless information and power transfer (SWIPT): Recent advances and future challenges," *IEEE Commun. Surveys Tuts.*, vol. 20, no. 1, pp. 264-302, Dec. 2017.

[6] H. Ju and R. Zhang, "Throughput maximization in wireless powered communication networks," *IEEE Trans. Wireless Commun.*, vol. 13, no. 1, pp. 418-428, Jan. 2014.

[7] H. Liu, F. Hu, S. Qu, Z. Li, and D. Li, "Multipoint wireless information and power transfer to maximize sum-throughput in WBAN with energy harvesting," *IEEE Internet Things J.*, vol. 6, no. 4, pp. 7069-7078, Aug. 2019.

[8] Z. Chu, T. A. Le, D. To, and H. X. Nguyen, "Sum throughput optimization for wireless powered sensor networks," in *Proc. IEEE GLOBECOM.,* Singapore, Dec. 2017, pp. 1-6.

[9] S. Shen, J. Qian, D. Cheng, K. Yang, and G. Zhang, "A sum-utility maximization approach for fairness resource allocation in wireless powered body area networks," *IEEE Access*, vol. 7, pp. 20014-20022, Feb. 2019.

[10] F. Yang, W. Xu, Z. Zhang, L. Guo, and J. Lin, "Energy efficiency maximization for relay-assisted WPCN: Joint time duration and power allocation," *IEEE Access*, vol. 6, pp. 78297-78307, Dec. 2018.

[11] Z. Mao, F. Hu, Z. Li, Z. Ling, and S. Li, "Energy-efficient optimization in multi-sensor WBAN with multi-antenna AP," *IEEE Access*, vol. 7, pp. 115409-115417, Jul. 2019.

[12] V. N. Vo, H. Tran, E. Uhlemann, Q. X. Truong, C. So-In, and A. Balador, "Reliable communication performance for energy harvesting wireless sensor networks," in *Proc. IEEE VTC,* Kuala Lumpur, Malaysia, 2019, pp. 1-6.

[13] K. Chi, Y.-H. Zhu, Y. Li, L. Huang, and M. Xia, "Minimization of transmission completion time in wireless powered communication networks," *IEEE Internet Things J.*, vol. 4, no. 5, pp. 1671-1683, Oct. 2017.

[14] G. J. Stigler, "The Adoption of the Marginal Utility Theory," *Hist. Polit. Econ.*, pp. 571-586, Sep. 1972.

[15] J. Yang and Q. Yang, "Power-delay tradeoff in wireless powered communication networks," *IEEE Trans. Veh. Technol.*, vol. 66, no. 4, pp. 3280-3292, Apr. 2017.

[16] Q. Wu, M. Tao, D. W. K. Ng, W. Chen, and R. Schober, "Energy-efficient resource allocation for wireless powered communication networks," *IEEE Trans. Wireless Commun.*, vol. 15, no. 3, pp. 2312-2327, Mar. 2016.

[17] Q. Wu, M. Tao, D. W. K. Ng, W. Chen, and R. Schober, "Energy-efficient transmission for wireless powered multiuser communication networks," in *Proc. IEEE ICC,* London, U.K., 2015, pp. 154-159.

[18] H. Ju and R. Zhang, "Optimal resource allocation in full-duplex wireless-powered communication network," *IEEE Trans. Commun.*, vol. 62, no. 10, pp. 3528-3540, Oct. 2014.

[19] Z. Yu, K. Chi, P. Hu, Y. Zhu, and X. Liu, "Energy provision minimization in wireless powered communication networks with node throughput requirement," *IEEE Trans. Veh. Technol.*, vol. 68, no. 7, pp. 7057-7070, Jul. 2019.

[20] J. Liu, K. Xiong, P. Fan, and Z. Zhong, "Resource allocation in wireless powered sensor networks with circuit energy consumption constraints," *IEEE Access*, vol. 5, pp. 22775-22782, Oct. 2017.

[21] B. Khalfi, B. Hamdaoui, M. B. Ghorbel, M. Guizani, X. Zhang, and N. Zorba, "Optimizing joint data and power transfer in energy harvesting multiuser wireless networks," *IEEE Trans. Veh. Technol.*, vol. 66, no. 12, pp. 10989-11000, Dec. 2017.

[22] Q. Wu, W. Chen, and J. Li, "Wireless powered communications with initial energy: QoS guaranteed energy-efficient resource allocation," *IEEE Commun. Lett.*, vol. 19, no. 12, pp. 2278-2281, Dec. 2015.

[23] Z. Ling, F. Hu, and M. Shao, "The optimal control policy for point-to-point wireless body area network based on simultaneous time-ratio and transmission power allocation," *IEEE Access*, vol. 7, pp. 46454-46460, Feb. 2019.

[24] X. Liu, F. Hu, M. Shao, D. Sui, and G. He, "Power allocation for energy harvesting in wireless body area networks," *China Commun.*, vol. 14, no. 6, pp. 22-31, Jun. 2017.

[25] S. Boyd and L. Vandenberghe, *Convex Optimization*, Cambridge: Cambridge Univ. Press, 2004.

[26] R. L. Burden, D. J. Faires, and A. M. Burden, *Numerical Analysis*, 10th ed., Boston: Cengage Learning, 2016.

[27] A. Astrin et al., "IEEE standard for local and metropolitan area networks-part 15.6: Wireless body area networks," IEEE Standard 802.15.6-2012, pp. 1-271, 2012.

[28] S. Timotheou, I. Krikidis, G. Zheng and B. Ottersten, "Beamforming for MISO interference channels with QoS and RF energy transfer," *IEEE Trans. Wireless Commun.*, vol. 13, no. 5, pp. 2646-2658, May 2014.

[29] A. F. Molisch, *Wireless Communications*, Hoboken: John Wiley & Sons Ltd., 2011.

[30] C. E. Shannon, "Communication in the presence of noise," in *Proc. IRE,* 1949, pp. 10-21.

[31] J. C. Kwan and A. O. Fapojuwo, "Radio frequency energy harvesting and data rate optimization in wireless information and power transfer sensor networks," *IEEE Sens. J.*, vol. 17, no. 15, pp. 4862-4874, Aug. 2017.

Tong Wang received the B.Eng. degree in electrical engineering and automation from Beihang University, Beijing, China, in 2006 and the M.Sc. degree (with distinction) in communications engineering and the Ph.D. degree in electronic engineering from the University of York, York, U.K., in 2008 and 2012, respectively. From 2012 to 2015, he was a Research Associate with the Institute for Theoretical Information Technology, RWTH Aachen University, Aachen, Germany. From 2014 to 2015, he was a Research Fellow of the Alexander von Humboldt Foundation. Since March 2016, he has been with the School of Electronics and Information Engineering, Harbin Institute of Technology, Shenzhen, China, where he is an Assistant Professor. His research interests include sensor networks, cooperative communications, adaptive filtering, and optimizations.

Yang Shen received the B.Eng. degree in communication engineering from Anhui University, Heifei, China, in 2018, and he is currently working toward the M.Eng. degree in electronic and communication engineering in Harbin Institute of Technology, Shenzhen, China. His research interests include wireless sensor networks and resource allocation.

Lin Gao (S'08-M'10-SM'16) is an Associate Professor with the School of Electronics and Information Engineering, Harbin Institute of Technology, Shenzhen, China. He received the Ph.D. degree in Electronic Engineering from Shanghai Jiao Tong University in 2010. His main research interests are in the area of network optimizations, game theory, and crowd intelligence, with particular focus on mobile crowd sensing, crowd computing, edge computing, and cognitive networking. He is the co-recipient of 4 Best Paper Awards from leading conference proceedings on wireless communications and networking. He received the IEEE ComSoc Asia-Pacific Outstanding Young Researcher Award in 2016.

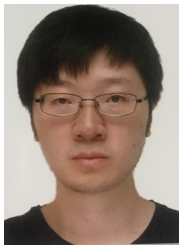

Yufei Jiang (S'12-M'14) received the Ph.D. degree in Electrical Engineering and Electronics from University of Liverpool, Liverpool, U.K., in 2014. From 2014 to 2015, he was a Postdoctoral Researcher with the Department of Electrical Engineering and Electronics, University of Liverpool. From 2015 to 2017, he was a Research Associate with the Institute for Digital Communications, University of Edinburgh, Edinburgh, U.K. He is currently an Assistant Professor with the Harbin Institute of Technology, Shenzhen, China. He received the best paper award at Globecom in 2019, and has served a number of conferences as TPC member, such as Globecom, ICC, PIMRC, VTC, WCSP and so on. His research interests include Li-Fi, synchronization, full-duplex, and blind source separation.

Ting Ma received the B.Eng. and M.Sc. degrees from the Harbin Institute of Technology (HIT), Harbin, China, in 1999 and 2001, respectively, and the Ph.D. degree in biomedical engineering from The Chinese University of Hong Kong (CUHK), Hong Kong, in 2004. From 2004 to 2009, she was a Postdoctoral Fellow with CUHK. From 2014 to 2016, she was a Visiting Professor with Johns Hopkins University. Since June 2009, she has been with the School of Electronics and Information Engineering, Harbin Institute of Technology at Shenzhen, Shenzhen, China, where she is currently an Associate Professor. Her research interests include neural computing, neural image processing, and brain informatics.

Xu Zhu (S'02-M'03-SM'12) received the B.Eng. degree (Hons.) in Electronics and Information Engineering from the Huazhong University of Science and Technology, Wuhan, China, in 1999, and the Ph.D. degree in Electrical and Electronic Engineering from The Hong Kong University of Science and Technology, HongKong, in 2003. She joined the Department of Electrical Engineering and Electronics, University of Liverpool, Liverpool, U.K., in 2003, as an Academic Member, where she is currently a Reader. She is also with the Harbin Institute of Technology, Shenzhen, China. She has more than 190 peer-reviewed publications on communications and signal processing. Her research interests include MIMO, channel estimation and equalization, resource allocation, cooperative communications, green communications etc.. She has acted as a Chair for various international conferences, such as the Vice-Chair of the 2006 and 2008 ICARN International Workshops, the Program Chair of ICSAI 2012, the Symposium Co-Chair of the IEEE ICC 2016, ICC 2019 and Globecom 2021, and the Publicity Chair of the IEEE IUCC 2016. She has served as an Editor for the IEEE Transactions on Wireless Communications and a Guest Editor for several international journals such as Electronics.